

# Computational and Experimental Approaches Identify Beta-Blockers as Potential SARS-CoV-2 Spike Inhibitors

Ana C. Puhl,\* Melina Mottin, Carolina Q. Sacramento, Tatyana Almeida Tavella, Gabriel Gonçalves Dias, Natalia Fintelman-Rodrigues, Jairo R. Temerozo, Suelen S. G. Dias, Paulo Ricardo Pimenta da Silva Ramos, Eric M. Merten, Kenneth H. Pearce, Fabio Trindade Maranhão Costa, Lakshmanane Premkumar, Thiago Moreno L. Souza, Carolina Horta Andrade,\* and Sean Ekins\*



Cite This: *ACS Omega* 2022, 7, 27950–27958



Read Online

ACCESS |



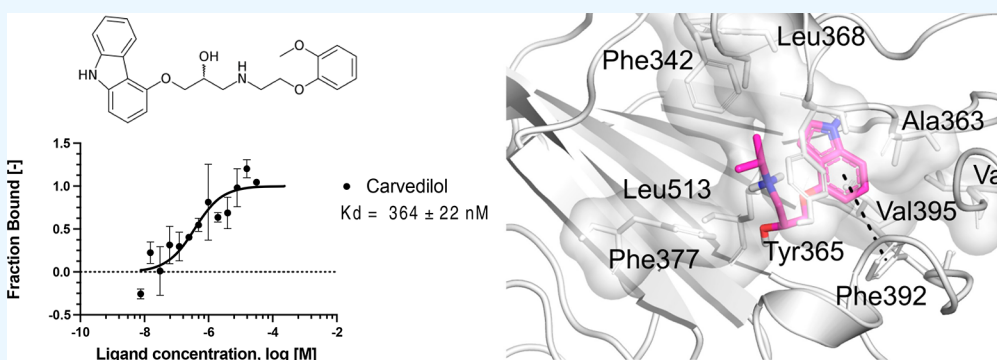
Metrics & More



Article Recommendations



Supporting Information



**ABSTRACT:** Finding antivirals for SARS-CoV-2 is still a major challenge, and many computational and experimental approaches have been employed to find a solution to this problem. While the global vaccination campaigns are the primary driver of controlling the current pandemic, orally bioavailable small-molecule drugs and biologics are critical to overcome this global issue. Improved therapeutics and prophylactics are required to treat people with circulating and emerging new variants, addressing severe infection, and people with underlying or immunocompromised conditions. The SARS-CoV-2 envelope spike is a challenging target for viral entry inhibitors. Pindolol presented a good docking score in a previous virtual screening using computational docking calculations after screening a Food and Drug Administration (FDA)-approved drug library of 2400 molecules as potential candidates to block the SARS-CoV-2 spike protein interaction with the angiotensin-converting enzyme 2 (ACE-2). Here, we expanded the computational evaluation to identify five beta-blockers against SARS-CoV-2 using several techniques, such as microscale thermophoresis, NanoDSF, and *in vitro* assays in different cell lines. These data identified carvedilol with a  $K_d$  of  $364 \pm 22$  nM for the SARS-CoV-2 spike and *in vitro* activity ( $EC_{50}$  of  $7.57 \mu\text{M}$ ,  $CC_{50}$  of  $18.07 \mu\text{M}$ ) against SARS-CoV-2 in Calu-3 cells. We have shown how we can apply multiple computational and experimental approaches to find molecules that can be further optimized to improve anti-SARS-CoV-2 activity.

## INTRODUCTION

The global efforts against the COVID-19 pandemic are still a challenge, with the emergence of new variants, and more than 569 million people have been infected with over 6 million deaths, while currently, more than 12 billion vaccine doses have been administered worldwide.<sup>1</sup> COVID-19 is caused by the betacoronavirus SARS-CoV-2 and was initially identified in Wuhan, China, in December 2019.<sup>2</sup> In addition to SARS-CoV-2, there are seven coronaviruses known to infect humans.<sup>3</sup> SARS-CoV-2 has propagated quickly worldwide and has caused considerable economic burden and stress on the global healthcare systems.<sup>4</sup> Among those showing symptoms of COVID-19, 5% developed a critical illness that progressed to

acute respiratory distress syndrome (ARDS), which can be fatal.<sup>2,5</sup> People who still have symptoms or complications after 4 weeks from the symptom onset are classified as having post-acute COVID-19 or long COVID-19.<sup>6,7</sup> COVID-19 is still a global concern, and due to the emergence of new variants and

Received: March 21, 2022

Accepted: July 15, 2022

Published: August 8, 2022



the relatively high mortality, developing coronavirus-specific therapeutics continues to be an urgent need.

In contrast, while garnering attention early in the epidemic, small-molecule drug discovery has not delivered that many promising clinical results. However, the Food and Drug Administration (FDA) authorized the emergency use of molnupiravir<sup>8</sup> and paxlovid.<sup>9</sup> Molnupiravir showed activity in several models of SARS-CoV-2, SARS-CoV-1, and middle east respiratory syndrome (MERS).<sup>10</sup> There has been much discussion of repurposing efforts to apply existing drugs to COVID-19, and remdesivir<sup>11</sup> was the first antiviral approved, while other drugs including the corticosteroid dexamethasone have also shown promising results in the clinic.<sup>12</sup> The computationally proposed kinase inhibitor baricitinib<sup>13</sup> was identified early on and validated *in vitro* and in patients.<sup>14</sup> Several types of computational approaches or high-throughput screens<sup>15</sup> have also identified other FDA-approved drugs with low micromolar activity. Currently, only a handful of drugs to treat COVID-19 are available, and they may still have a long way to go into the research and development process.

The spike protein of the SARS-CoV-2 is one of the main targets to develop vaccines for SARS-CoV-2. This protein is composed of a trimeric protein that binds to the angiotensin-converting enzyme 2 (ACE2) receptor, and this interaction is the first step of virus entry.<sup>16</sup> High-affinity miniprotein binders for the receptor-binding domain (RBD) have been discovered by computational design<sup>17</sup> and numerous nanobodies and neutralizing antibodies that bind to the spike RBD.<sup>18</sup>

In a previous study, we described a docking-based virtual screen of FDA-approved drugs (~2400 molecules), targeting the interaction between the SARS-CoV-2 spike RBD and the host ACE2, and identified pindolol as a potential hit.<sup>19</sup> We have now experimentally evaluated this drug and four other beta-blockers. Here, we demonstrate the discovery of these additional compounds that represent starting points to optimize affinity for an inhibitor or as development probes to be used in new assays to study SARS-CoV-2.

## ■ EXPERIMENTAL SECTION

**Compound/Chemical Sources.** Pindolol, carvedilol, carteolol, atenolol, and  $\pm$ bisoprolol were purchased from MedChemExpress (MCE, Monmouth Junction, NJ).

**Microscale Thermophoresis.** To study the interaction of compounds with the SARS-CoV-2 spike RBD (331–528 amino acids),<sup>20</sup> we employed microscale thermophoresis (MST) as described by our group,<sup>21,22</sup> using MST buffer (HEPES 10 mM pH 7.4, NaCl 150 mM) and the Monolith Protein Labeling Kit RED-NHS 2nd Generation kit (Amine Reactive).

**Nanodifferential scanning fluorimetry (nanoDSF).** NanoDSF experiments were conducted using the Nanotemper Prometheus NT.48 system. The SARS-Cov-2 spike RBD was diluted to 5  $\mu$ M in phosphate-buffered saline (PBS) at pH 7.4 and incubated with 100  $\mu$ M of each compound. We performed thermal denaturation experiments from 15 to 95 °C at 1 °C/min. Nanotemper PR.Thermocontrol software was used to automatically calculate the melting temperature ( $T_m$ ). We reported the fluorescence ratio at 330:350 nm wavelength.

**Homogeneous Bioluminescent SARS-CoV-2 Spike RBD: ACE2 Immunoassay.** We tested if the compounds could disrupt the interaction between the spike RBD and ACE2 using the kit Lumit SARS-CoV-2 spike RBD: hACE2 Immunoassay<sup>23</sup> (Promega), following the manufacturer's

instructions. Briefly, 100 nL of compounds of interest in 100% dimethyl sulfoxide (DMSO) was added to the plate using a Mosquito HTS; 100 nL of 100% DMSO was added to control wells, and 0.9  $\mu$ L of buffer C (Promega) was added to all sample and control wells. For the positive control, 0.9  $\mu$ L of 1.7  $\mu$ M His-RBD was added to the wells. After this, 2  $\mu$ L of the 7.5 nM rFc-RBD reagent was added to all wells. A total of 2  $\mu$ L of 7.5 nM mFc-ACE2 was added to all wells, followed by 5  $\mu$ L of Lumit antibody mix to all wells, and the plate was kept on a plate shaker at low speed for 1 min and then centrifuged at 1000 RPM for 2 min. After 60 min, 2.5  $\mu$ L of the Lumit detection reagent was dispensed to all wells. The plate was maintained at 25 °C for 30 min, and the luminescence was read in a EnVision 2103 multilabel plate reader (PerkinElmer).

**Cell Culture.** The cellular lines from human epithelial lung carcinoma (A549) and the African green monkey kidney (Vero, subtype E6) were cultured in high-glucose Dulbecco's modified Eagle medium (DMEM) supplemented with 10% fetal bovine serum (FBS; HyClone), 100 U/mL penicillin, and 100  $\mu$ g/mL streptomycin (P/S). Cells were maintained with 5% CO<sub>2</sub> at 37 °C. The SARS-CoV-2 (GenBank #MT710714) was grown in Vero E6 cells at a multiplicity of infection (MOI) of 0.01. Virus titers were determined as plaque-forming units (PFU); PFU/mL was used for virus titer determination. Virus stocks were stored at –80 °C.

**CC<sub>50</sub> Determination in Vero and A549 Cells.** The 3-(4,5-dimethylthiazol-2-yl)-2,5-diphenyl-2H-tetrazolium bromide (MTT) assay was used to determine the cytotoxicity of compounds, as described.<sup>22</sup> Briefly, Vero or A549 cells were cultivated at 5% CO<sub>2</sub> and 37 °C using Dulbecco's modified Eagle medium supplemented with 10% heat-inactivated fetal bovine serum. A549 or Vero cells at a density of 10<sup>4</sup> cells/well were cultivated in a 96-well plate prior to incubation with compounds for 72 h. Cellular viability was calculated as a percentage in comparison to the vehicle control.

**Adsorption Inhibition Assays.** SARS-CoV-2 or Vero E6 cells (5  $\times$  10<sup>5</sup> cells/well in 48-well plates) were preincubated with 1  $\mu$ M of the tested compounds for 1 h at 37 °C. Subsequently, the cells were infected with SARS-CoV-2 for 1 h at 4 °C, a condition that allows only the virus to adsorb. The supernatant was removed, and the cells were rinsed twice with PBS. Total viral RNA extraction from cell lysate and the quantitative real-time polymerase chain reaction (RT-PCR) were conducted as described previously.<sup>24</sup>

**Calu-3 Assays.** The experiments with Calu-3 (ATCC, HTB-55) were conducted as described previously.<sup>22</sup> DMSO wells are the negative controls, and the compound data were normalized to DMSO.

**Molecular Docking Calculations.** We used the DockThor VS web server<sup>25</sup> to perform docking calculations at the spike linoleic acid (LA)-binding site.<sup>26</sup> We used the Protein Preparation Wizard tool<sup>27,28</sup> and LigPrep tool<sup>28</sup> to prepare the three-dimensional (3D) protein structure, PDB ID 6ZB5<sup>26</sup> (chain A of the RBD, residues from 331 to 528), and beta-blocker molecular structures, respectively. The docking grid was centered at the LA-binding site,<sup>26</sup> with a grid size of 20 Å and grid coordinates  $x$ ,  $y$ , and  $z$  of 122, 96, 152 Å, respectively. The standard configuration of genetic algorithm parameters and the soft docking mode were used. Then, we used the PLIP<sup>29</sup> server to analyze the protein–ligand patterns of the interaction of the docking poses. For figures, we used Pymol.<sup>30</sup>

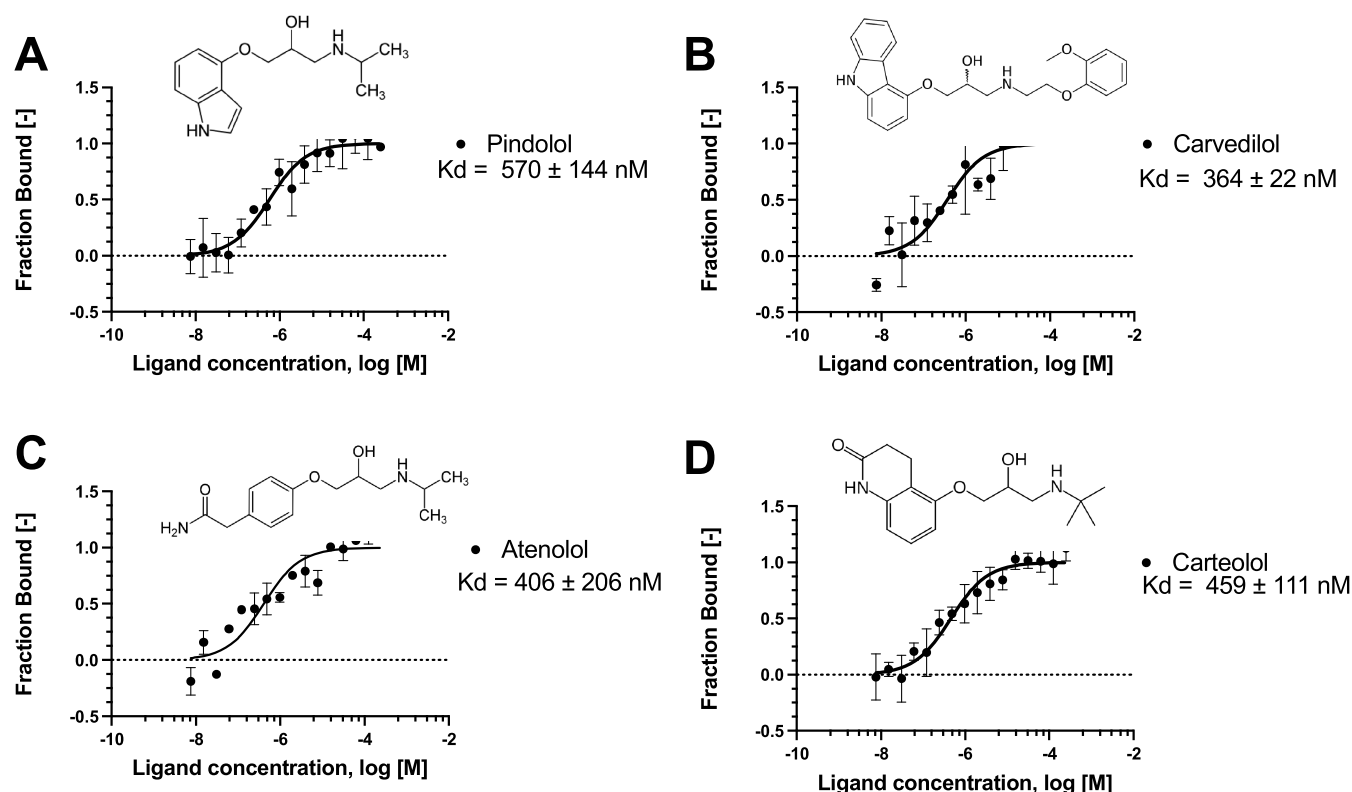


**Figure 1.** Microscale thermophoresis for the interaction between the spike RBD and compounds. (A) Pindolol, (B) carvedilol, (C) atenolol, and (D) carteolol. The labeled spike RBD at 5 nM was incubated with the compounds, in the concentration range from 250  $\mu$ M to 7.629 nM. The curve is shown as fraction bound [-] against the compound concentration on a log scale.

## RESULTS

**Spike RBD.** In our previous work,<sup>19</sup> we described the docking study of FDA-approved drugs (~2400 molecules) against the interface of the SARS-CoV-2 spike 3D model (obtained by homology) and the ACE2. Despite only highlighting four drugs in that publication,<sup>19</sup> pindolol presented a good docking score, and we have since identified it as a potential ligand of the spike RBD–ACE2 interface. Here, we have used MST to verify the interaction of pindolol with the spike RBD ( $K_d$  570  $\pm$  144 nM, Figure 1). We further evaluated other beta-blockers such as carvedilol, carteolol, and atenolol using MST and found that they have  $K_d$  values of 364  $\pm$  22, 459  $\pm$  111, and 406  $\pm$  206 nM, respectively (Figure 1). These compounds did not promote significant changes in the melting temperature ( $T_m$ ) using nanoDSF (Table S1).

Pindolol, carteolol,  $\pm$ bisoprolol, and carvedilol were evaluated in a Lumit SARS-CoV-2 spike RBD: hACE2 Immunoassay<sup>23</sup> (Promega), to verify if these compounds could disrupt the interaction between the RBD and ACE2. In addition to beta-blockers, we also tested linoleic acid, which was reported to bind to the spike.<sup>26</sup> None of the compounds tested were able to disrupt the interaction (Figure S1).

**Cell-Based Assays.** We evaluated the cytotoxic effects of the various compounds on two mammalian cell lines, Vero E6 and A549. Cytotoxicity was determined using the MTT assay (Table S2). Furthermore, we functionally evaluated in Vero E6 cells whether the compounds would block the spike protein through adsorption inhibition assays. Cells were infected with SARS-CoV-2 preincubated or not with the compounds for 1 h at 4  $^{\circ}$ C, a condition that allows only the virus to adsorb. We used three experimental conditions, one in which cells were

incubated with 1  $\mu$ M compounds prior to SARS-CoV-2 infection, another where viruses were incubated with 1  $\mu$ M compounds prior to cellular infection, and a condition evaluating both, where viruses and compounds were added simultaneously to the cells. Figure 2 shows that carvedilol, atenolol, and bisoprolol statistically decreased SARS-CoV-2 adsorption to the cells only when viruses were preincubated with the compounds.

Among the compounds tested in the adsorption assay, cells treated with carvedilol showed the highest reduction on SARS-

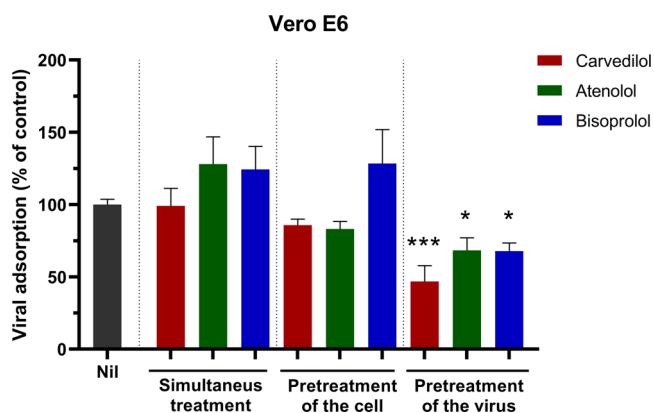


**Figure 2.** Reduction of SARS-CoV-2 entry in Vero E6 cells. SARS-CoV-2 and Vero E6 cells were pretreated (or not) with the beta-blockers for 1 h at 37  $^{\circ}$ C. Then, pretreated or untreated cells and virus were incubated together for 1 h at 4  $^{\circ}$ C. Viral RNA quantification by RT-PCR on cell lysates. Results are shown as a percentage of SARS-CoV-2 adsorption. Nil: infected and nontreated.

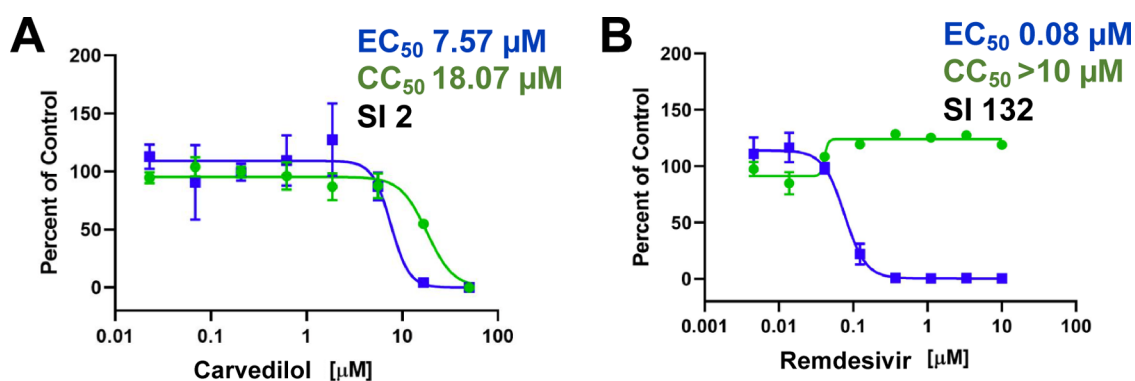


**Figure 3.** Carvedilol (A) and remdesivir (B) were tested in Calu-3 cells. Calu-3 (ATCC, HTB-55) cells were pretreated with test compounds for 2 h prior to continuous infection with SARS-CoV-2 (isolate USA WA1/2020) at MOI = 0.5. Cells were imaged 48 h after infection.  $EC_{50}$  (infection: blue) and  $CC_{50}$  (toxicity: green).

CoV-2 adsorption, and this compound was selected for further testing in Calu-3 cells infected with SARS-CoV-2, where the cells were pretreated with the compound for 2 h prior to infection. Carvedilol had an  $EC_{50}$  of 7.57  $\mu\text{M}$ ,  $CC_{50}$  of 18.07  $\mu\text{M}$ , and SI of 2 (Figure 3A). Remdesivir had an  $EC_{50}$  of 0.08  $\mu\text{M}$  and  $CC_{50}$  > 10  $\mu\text{M}$  (Figure 3B). \*  $P < 0.05$  and \*\*\* $P < 0.001$ .

**Molecular Docking Calculations.** We performed docking calculations of the selected beta-blockers at the fatty acid-binding site of the spike protein to investigate how the beta-blockers might interact with the spike. The literature describes this region as a potential site for binding putative inhibitors.<sup>26,31</sup> The spike RBD–ACE2 interface was used as a binding site for docking calculations in our previous work but was not investigated here due to its flat shape, and therefore, it is not considered an ideal binding site for small molecules. The docking scores for carvedilol, carteolol, pindolol, and atenolol were favorable,  $-11.3$ ,  $-9.4$ ,  $-9.4$ , and  $-8.8$  Kcal·mol<sup>-1</sup>, respectively. Linoleic acid showed a docking score of  $-9.5$  Kcal·mol<sup>-1</sup> and RMSD value of 1.8 Å in the redocking calculations, and in comparison with this result, the beta-blockers presented promising results at the linoleic acid-binding site in our docking simulations. The ligand–protein interactions of docking poses showed that the compounds could be interacting in the linoleic acid-binding site mainly with several hydrophobic residues and established several  $\pi$ -stacking and hydrophobic interactions (Figure 4).

In the crystallographic structure PDB ID 6ZB5, linoleic acid made hydrophobic interactions with Ala363, Tyr365, Phe374, Phe392, Val395, Leu513, and Phe515. In our docking calculations, the beta-blockers made several similar interactions as linoleic acid and additional ones in the linoleic acid-binding site. In general, the hydrophobic moiety of beta-blockers fits the hydrophobic aliphatic moiety of the linoleic acid molecule. Moreover, carvedilol had the best docking score and was predicted to make  $\pi$ -stacking interactions with Phe374 and Phe392 and hydrophobic interactions with the Tyr369 residue (at the gating helix) (Figure 4A). Carteolol was predicted to make hydrophobic interactions with Tyr365 (gating helix), Phe374, Phe392, Leu513, and Phe515 (Figure 4B). Pindolol was predicted to make hydrophobic interactions with Ala363, Tyr365 (gating helix), Val365, and Leu513 and  $\pi$ -stacking interactions with Phe392 (Figure 4C). Atenolol was predicted to make hydrophobic interactions with Ala363, Leu513, and Phe515 and  $\pi$ -stacking interactions with Phe374 (Figure 4D). Toelzer and co-workers<sup>26</sup> had previously highlighted the

importance of Tyr365 and Tyr369 for the gating helix, whose opening allows the accommodation of the linoleic acid molecule into the spike RBD. Our docking results showed that all investigated beta-blockers may interact with the gating helix residues, which can lead to a better fit in the site. In Figure 4E, we show that all the beta-blockers superimposed on the linoleic acid molecule, highlighting the generally similar alignment of their binding modes.

## DISCUSSION

In our previous work,<sup>19</sup> we initially focused our attention on drugs that might impair the interaction between the SARS-CoV-2 spike and host ACE2 docking compounds from a FDA-approved drug library.<sup>19</sup> We suggested pindolol as a possible ligand targeting the RBD–ACE2 interface. However, at that time, we used a 3D model of the RBD spike modeled by homology with limited knowledge of the spike binding sites. Now, we have tested several predictions and screened compounds by measuring the binding affinity of the compounds to the spike RBD using MST. We initially identified pindolol as a potential ligand of the spike RBD and subsequently measured the affinity of carvedilol, atenolol, and carteolol using MST. Figure 1 shows how these beta-blockers (which are used to treat high blood pressure) may bind to the SARS-CoV-2 spike RBD protein including pindolol, carvedilol, carteolol, and atenolol, suggesting that they could potentially bind to the interface between the spike RBD and ACE2.<sup>36</sup> The docking calculations with the series of beta-blockers showed that they may interact in the fatty acid-binding site of the spike with satisfactory binding affinities (docking scores ranging from  $-11.3$  to  $-8.8$  Kcal·mol<sup>-1</sup>), interacting with the gating helix (an important region that allows ligand accommodation) and showing similar interactions as observed for the linoleic acid present in the spike Cryo-EM structure<sup>26</sup> (Figure 4E). In addition, new structures of the spike protein interacting with the 9-octadecenoid acid deposited were in the Protein Data Bank (PDB ID 7E7B, 7E7D),<sup>32</sup> showing similar interactions with spike residues and a comparable binding mode with the spike–linoleic acid complex structure. Toelzer and co-workers<sup>26</sup> suggested that linoleic acid binding stabilizes the spike in a locked conformation (RBD down), reducing the spike–ACE2 interaction *in vitro*. Our docking predictions, at the same binding site as linoleic acid, suggest that the beta-blockers could also have implications for the spike–ACE2 interaction.

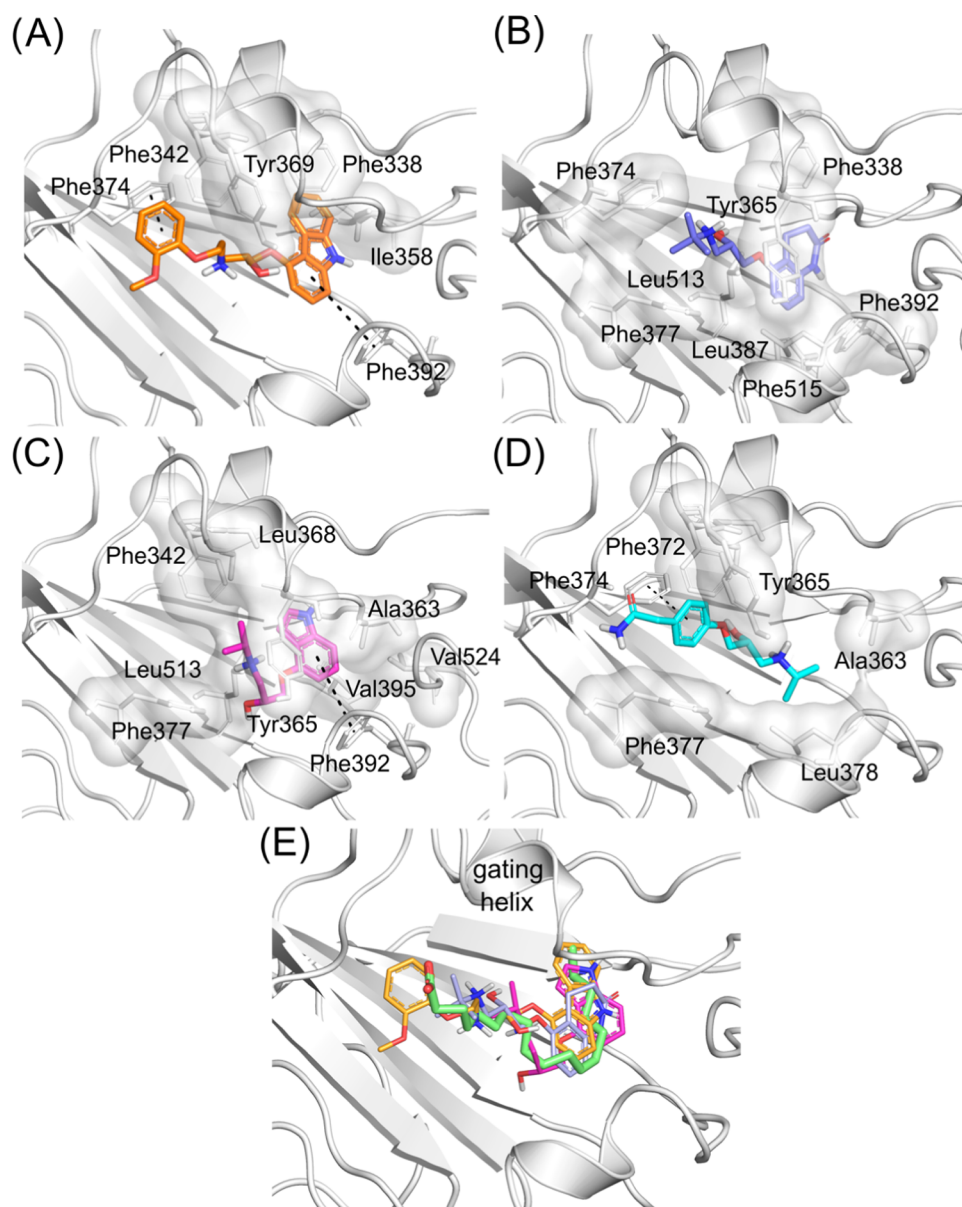


**Figure 4.** 3D intermolecular interactions of the SARS-CoV-2 spike at the fatty acid site with (A) carvedilol (carbons colored in orange), (B) carteolol (carbons colored in blue), (C) pindolol (carbons colored in magenta), and (D) atenolol (carbons colored in cyan). Hydrogen, nitrogen, and oxygen atoms are colored in white, blue, and red, respectively. Hydrophobic interactions are shown as a white transparent surface, and  $\pi$ -stacking interactions are shown as green dotted lines. (E) Superposition of beta-blocker docking poses with the linoleic acid from the crystal structure (PDB ID 6ZB5) (carbons colored in green).

We evaluated cytotoxicity in Vero and A549 cells (Table S2) and determined an optimal concentration to test in cells infected with SARS-CoV-2. We then demonstrated that the compounds would block the spike protein through adsorption inhibition assays in Vero E6 cells and that carvedilol, atenolol, and bisoprolol statistically reduced SARS-CoV-2 adsorption to the cells when the virus was pretreated with the compounds (Figure 2). This may potentially demonstrate that compounds bind to the RBD or another spike region; however, in our MST experiments, bisoprolol did not bind to the RBD spike (data not shown). When the compounds and virus were added at the same time to the cells, we did not see any effect in blocking infection. This could also be explained by the high affinity of the spike RBD to the ACE2, which was previously reported to be  $\sim 15$  nM,<sup>40</sup> while the beta-blockers showed a  $K_d$  of  $> 300$  nM (Figure 1).

When incubation of virus and cells was conducted at the same time, the affinity of ACE2 to the spike RBD is much higher, and we do not observe an effect of the compounds blocking that interaction at the concentration of compounds tested ( $1 \mu\text{M}$ ). We further investigated pindolol, carteolol,  $\pm$ bisoprolol, and carvedilol using a bioluminescence Lumit screen assay to verify if these compounds could disrupt the interaction between the RBD and ACE2; however, none of the compounds tested were able to disrupt the interaction (Figure S1). This might also confirm that despite binding to the RBD, the affinity of these compounds is insufficient to compete with ACE2 or they might be binding to a site that cannot disrupt the interaction with ACE2. Despite a structure of the spike RBD which has been reported in the presence of linoleic acid,<sup>26</sup> in the Lumit assay, this fatty acid was not able to disrupt the interaction between ACE2 and the RBD (Figure S1).

However, the Lumit assay might pose some limitations because we are only using the spike RBD and not the spike trimer, which was the structure used in the presence of linoleic acid for the published structure. We have recently identified a dataset of compounds screened for SARS-CoV-2 in Vero cells available on ChEMBL<sup>33</sup> (ChEMBL4303835), where atenolol showed 25.84% inhibition of SARS-CoV-2-induced cytotoxicity of Caco-2 cells at 10  $\mu\text{M}$  after 48 h, carvedilol did not show activity, and carteolol and bisoprolol were not tested.<sup>34</sup>

The SARS-CoV-2 spike RBD has been shown to bind to ACE2 with a higher affinity compared to SARS-CoV<sup>40</sup>. If the entry of SARS-CoV-2 into host cells could be blocked by impairing the interaction of the spike protein with the ACE2 receptor, it could represent a potential strategy against COVID-19; however, with numerous mutations on the spike leading to new variants (such as Omicron), it might pose a challenge for the development of new antivirals targeting the spike alone. Here, we report some molecules that could be used as a starting point to design inhibitors or to develop assays to study the spike RBD that could be used to block virus entry.

Inhibitors of the spike protein–ACE2 interaction have been identified previously including cliquinol in Vero cells ( $\text{EC}_{50}$  of 12.62  $\mu\text{M}$ ), and this was also found to inhibit the exopeptidase activity ( $\text{IC}_{50}$  of 5.36  $\mu\text{M}$ ).<sup>35</sup> Quercetin was identified by others as an inhibitor of this target ( $\text{IC}_{50}$  of 7  $\mu\text{M}$ ),<sup>36</sup> but it was not tested against virally infected cells. Several of the compounds we have assessed were tested in Vero E6 cells, and we observed that carvedilol, atenolol, and bisoprolol were able to reduce SARS-CoV-2 adsorption into Vero cells through real-time RT-PCR; however, bisoprolol did not bind at the spike RBD, but in our MST and Lumit assay experiments, we only use a monomer and not the spike trimer. We also performed inhibition assays with Calu-3 to test the activity of carvedilol, which showed an  $\text{EC}_{50}$  of 7.57  $\mu\text{M}$ ,  $\text{CC}_{50}$  of 18.07  $\mu\text{M}$ , and SI of 2 (Figure 3A).

Since the discovery of SARS-CoV-2, there have been hundreds of papers describing computational or *in vitro* screening approaches, proposing compounds with likely activity against this virus. The most relevant are those in which compounds are tested *in vitro* in infected cells with activity in the low-nM– $\mu\text{M}$  range. We have recently demonstrated sub-micromolar activities for tilorone, pyronaridine, and quinacrine in A549-ACE2 cells,<sup>22</sup> and pyronaridine has demonstrated efficacy in a mouse model infected with SARS-CoV-2.<sup>37</sup> Both tilorone<sup>38</sup> and pyronaridine (NCT05084911) have also progressed to clinical trials.

With the continual increase in new variant SARS-CoV-2 strains,<sup>39</sup> there is a critical need to accelerate the development of treatments that could be effective for COVID-19. Small-molecule drugs orally administered present several advantages, as they are easily accessible outside hospitals and are also more stable for storage (unlike the current vaccines and antibody treatments). In this study, we have used several techniques, such as docking, MST, nanoDSF, and cell assays, to identify and characterize inhibitors of the spike protein. We have now validated our prediction from the earliest stages of the pandemic, which proposes that beta-blockers may be useful starting points to design molecules that can bind to the SARS-CoV-2 spike protein.<sup>19</sup> Future work may include testing carvedilol or analogues in animal models infected with SARS-CoV-2. It will also be of interest to assess clinical data from patients treated with beta-blockers and analyze whether they

had lower infection rates with COVID-19 during the pandemic.

## ■ ASSOCIATED CONTENT

### Supporting Information

The Supporting Information is available free of charge at <https://pubs.acs.org/doi/10.1021/acsomega.2c01707>.

NanoDSF, Lumit assay, and cytotoxicity data of compounds tested (PDF)

## ■ AUTHOR INFORMATION

### Corresponding Authors

Ana C. Puhl – Collaborations Pharmaceuticals, Inc., Raleigh, North Carolina 27606, United States; [orcid.org/0000-0002-1456-8882](https://orcid.org/0000-0002-1456-8882); Email: [ana@collaborationspharma.com](mailto:ana@collaborationspharma.com)

Carolina Horta Andrade – LabMol - Laboratory of Molecular Modeling and Drug Design, Faculdade de Farmácia, Universidade Federal de Goiás, Goiânia 74605-170 GO, Brazil; [orcid.org/0000-0003-0101-1492](https://orcid.org/0000-0003-0101-1492); Email: [carolina@ufg.br](mailto:carolina@ufg.br)

Sean Ekins – Collaborations Pharmaceuticals, Inc., Raleigh, North Carolina 27606, United States; [orcid.org/0000-0002-5691-5790](https://orcid.org/0000-0002-5691-5790); Phone: +1 215-687-1320; Email: [sean@collaborationspharma.com](mailto:sean@collaborationspharma.com)

### Authors

Melina Mottin – LabMol - Laboratory of Molecular Modeling and Drug Design, Faculdade de Farmácia, Universidade Federal de Goiás, Goiânia 74605-170 GO, Brazil; Pathogen-Host Interface Laboratory, Department of Cell Biology, University of Brasilia, Brasilia 70910-900, Brazil

Carolina Q. Sacramento – Laboratory of Immunopharmacology, Oswaldo Cruz Institute—Fiocruz, Rio de Janeiro 21040-360 RJ, Brazil; Center of Technological Development in Health (CDTS)/National Institute of Science and Technology for Innovation on Neglected Population Diseases (INCT-IDPN), Rio de Janeiro 21040-900 RJ, Brazil

Tatyana Almeida Tavella – Laboratory of Tropical Diseases—Prof. Dr. Luiz Jacinto da Silva, Department of Genetics, Evolution, Microbiology and Immunology, University of Campinas-UNICAMP, Campinas 13083-970 SP, Brazil

Gabriel Gonçalves Dias – LabMol - Laboratory of Molecular Modeling and Drug Design, Faculdade de Farmácia, Universidade Federal de Goiás, Goiânia 74605-170 GO, Brazil

Natalia Fintelman-Rodrigues – Laboratory of Immunopharmacology, Oswaldo Cruz Institute—Fiocruz, Rio de Janeiro 21040-360 RJ, Brazil; Center of Technological Development in Health (CDTS)/National Institute of Science and Technology for Innovation on Neglected Population Diseases (INCT-IDPN), Rio de Janeiro 21040-900 RJ, Brazil

Jairo R. Temerozo – Laboratory on Thymus Research, Oswaldo Cruz Institute—Fiocruz, Rio de Janeiro 21040-900 RJ, Brazil; National Institute for Science and Technology on Neuroimmunomodulation (INCT/NIM), Oswaldo Cruz Institute—Fiocruz, Rio de Janeiro 21040-360 RJ, Brazil

Suelen S. G. Dias – Laboratory of Immunopharmacology, Oswaldo Cruz Institute—Fiocruz, Rio de Janeiro 21040-360 RJ, Brazil

Paulo Ricardo Pimenta da Silva Ramos – *LabMol - Laboratory of Molecular Modeling and Drug Design, Faculdade de Farmácia, Universidade Federal de Goiás, Goiânia 74605-170 GO, Brazil*

Eric M. Merten – *Center for Integrative Chemical Biology and Drug Discovery, Chemical Biology and Medicinal Chemistry, Eshelman School of Pharmacy, University of North Carolina, Chapel Hill, North Carolina 27599, United States*

Kenneth H. Pearce – *Center for Integrative Chemical Biology and Drug Discovery, Chemical Biology and Medicinal Chemistry, Eshelman School of Pharmacy, University of North Carolina, Chapel Hill, North Carolina 27599, United States; UNC Lineberger Comprehensive Cancer Center, Chapel Hill, North Carolina 27599, United States*

Fabio Trindade Maranhão Costa – *Laboratory of Tropical Diseases—Prof. Dr. Luiz Jacinto da Silva, Department of Genetics, Evolution, Microbiology and Immunology, University of Campinas-UNICAMP, Campinas 13083-970 SP, Brazil*

Lakshmanane Premkumar – *Department of Microbiology and Immunology, University of North Carolina School of Medicine, Chapel Hill, North Carolina 27599, United States*

Thiago Moreno L. Souza – *Laboratory of Immunopharmacology, Oswaldo Cruz Institute—Fiocruz, Rio de Janeiro 21040-360 RJ, Brazil; Center of Technological Development in Health (CDTS)/National Institute of Science and Technology for Innovation on Neglected Population Diseases (INCT-IDPN), Rio de Janeiro 21040-900 RJ, Brazil*

Complete contact information is available at:  
<https://pubs.acs.org/10.1021/acsomega.2c01707>

## Funding

The authors acknowledge NIH funding R44GM122196-02A1 from NIGMS (PI – S.E.) and 1R43AT010585-01 from NIH/NCCAM and the Brazilian funding agencies FAPESP 2019/27626-3 – (T.A.T. fellowship), 2020/05369-6 (F.T.M.C. grant); FAPEG (PI – C.H.A., 202010267000272), CNPq (PI – C.H.A., 441038/2020-4); and CNPq 150636/2020-2 and CAPES 88887.510530/2020-00 (M.M.). This project was also supported by the North Carolina Policy Collaboratory at the University of North Carolina at Chapel Hill with funding from the North Carolina Coronavirus Relief Fund established and appropriated by the North Carolina General Assembly. Collaborations Pharmaceuticals, Inc. has utilized the non-clinical and preclinical service program offered by the National Institute of Allergy and Infectious Diseases.

## Notes

The authors declare the following competing financial interest(s): SE is CEO of Collaborations Pharmaceuticals, Inc. ACP is an employee at Collaborations Pharmaceuticals, Inc.

S.E. is the CEO of Collaborations Pharmaceuticals, Inc. A.C.P. is an employee at Collaborations Pharmaceuticals, Inc.

## ACKNOWLEDGMENTS

Dr. Mindy Davis and colleagues gratefully acknowledge the assistance with the NIAID virus screening capabilities. The authors graciously thank Dr. Sara Cherry and Dr. David Schultz for the Calu-3 high-content SARS-CoV-2 studies performed by the University of Pennsylvania High-Throughput Screening Core and the Cherry Laboratory. The authors also

wish to thank Dr. Dinorah Leyva (NanoTemper) for assistance with MST data analysis.

## ABBREVIATIONS USED

ACE-2:angiotensin-converting enzyme 2; RBD:receptor-binding domain; MST:microscale thermophoresis; nanoDSF:nanoscale differential scanning fluorimetry

## REFERENCES

- (1) Anon. COVID-19 Dashboard, 2022. <https://coronavirus.jhu.edu/map.html> (accessed April 27, 2022).
- (2) Yang, X.; Yu, Y.; Xu, J.; Shu, H.; Xia, J.; Liu, H.; Wu, Y.; Zhang, L.; Yu, Z.; Fang, M.; et al. Clinical course and outcomes of critically ill patients with SARS-CoV-2 pneumonia in Wuhan, China: a single-centered, retrospective, observational study. *Lancet Respir. Med.* **2020**, *8*, 475–481.
- (3) (a) Jo, W. K.; Drosten, C.; Drexler, J. F. The evolutionary dynamics of endemic human coronaviruses. *Virus Evol.* **2021**, *7*, No. veab020. (b) Zhu, Z.; Lian, X.; Su, X.; Wu, W.; Marraro, G. A.; Zeng, Y. From SARS and MERS to COVID-19: a brief summary and comparison of severe acute respiratory infections caused by three highly pathogenic human coronaviruses. *Respir. Res.* **2020**, *21*, No. 224.
- (4) Shang, Y.; Li, H.; Zhang, R. Effects of Pandemic Outbreak on Economies: Evidence From Business History Context. *Front. Public Health* **2021**, *9*, No. 632043.
- (5) (a) Huang, C.; Wang, Y.; Li, X.; Ren, L.; Zhao, J.; Hu, Y.; Zhang, L.; Fan, G.; Xu, J.; Gu, X.; et al. Clinical features of patients infected with 2019 novel coronavirus in Wuhan, China. *Lancet* **2020**, *395*, 497–506. (b) Wang, C.; Wang, Z.; Wang, G.; Lau, J. Y.; Zhang, K.; Li, W. COVID-19 in early 2021: current status and looking forward. *Signal Transduction Targeted Ther.* **2021**, *6*, No. 114.
- (6) (a) Nalbandian, A.; Sehgal, K.; Gupta, A.; Madhavan, M. V.; McGroder, C.; Stevens, J. S.; Cook, J. R.; Nordvig, A. S.; Shalev, D.; Sreerawat, T. S.; et al. Post-acute COVID-19 syndrome. *Nat. Med.* **2021**, *27*, 601–615. (b) Huang, C.; Huang, L.; Wang, Y.; Li, X.; Ren, L.; Gu, X.; Kang, L.; Guo, L.; Liu, M.; Zhou, X.; et al. 6-month consequences of COVID-19 in patients discharged from hospital: a cohort study. *Lancet* **2021**, *397*, 220–232.
- (7) Silva Andrade, B.; Siqueira, S.; de Assis Soares, W. R.; de Souza Rangel, F.; Santos, N. O.; Dos Santos Freitas, A.; Ribeiro da Silveira, P.; Tiwari, S.; Alzahrani, K. J.; Góes-Neto, A.; et al. Long-COVID and Post-COVID Health Complications: An Up-to-Date Review on Clinical Conditions and Their Possible Molecular Mechanisms. *Viruses* **2021**, *13*, No. 700.
- (8) Jayk Bernal, A.; Gomes da Silva, M. M.; Musungaie, D. B.; Kovalchuk, E.; Gonzalez, A.; Delos Reyes, V.; Martín-Quirós, A.; Caraco, Y.; Williams-Diaz, A.; Brown, M. L.; et al. Molnupiravir for Oral Treatment of Covid-19 in Nonhospitalized Patients. *N. Engl. J. Med.* **2022**, *386*, 509–520.
- (9) Owen, D. R.; Allerton, C. M. N.; Anderson, A. S.; Aschenbrenner, L.; Avery, M.; Berritt, S.; Boras, B.; Cardin, R. D.; Carlo, A.; Coffman, K. J.; et al. An oral SARS-CoV-2 M. *Science* **2021**, *374*, 1586–1593.
- (10) (a) Sheahan, T. P.; Sims, A. C.; Zhou, S.; Graham, R. L.; Puijssers, A. J.; Agostini, M. L.; Leist, S. R.; Schafer, A.; Dinnon, K. H., 3rd; Stevens, L. J.; et al. An orally bioavailable broad-spectrum antiviral inhibits SARS-CoV-2 in human airway epithelial cell cultures and multiple coronaviruses in mice. *Sci. Transl. Med.* **2020**, *12*, No. eabb5883. (b) Wahl, A.; Gralinski, L. E.; Johnson, C. E.; Yao, W.; Kovarova, M.; Dinnon, K. H., 3rd; Liu, H.; Madden, V. J.; Krzystek, H. M.; De, C.; et al. SARS-CoV-2 infection is effectively treated and prevented by EIDD-2801. *Nature* **2021**, *591*, 451–457. (c) Rosenke, K.; Hansen, F.; Schwarz, B.; Feldmann, F.; Haddock, E.; Rosenke, R.; Barbian, K.; Meade-White, K.; Okumura, A.; Leventhal, S.; et al. Orally delivered MK-4482 inhibits SARS-CoV-2 replication in the Syrian hamster model. *Nat. Commun.* **2021**, *12*, No. 2295. (d) Anon. Merck and Ridgeback's Investigational Oral Antiviral Molnupiravir

Reduced the Risk of Hospitalization or Death by Approximately 50 Percent Compared to Placebo for Patients with Mild or Moderate COVID-19 in Positive Interim Analysis of Phase 3 Study, 2021. <https://www.merck.com/news/merck-and-ridgebacks-investigational-oral-antiviral-molnupiravir-reduced-the-risk-of-hospitalization-or-death-by-approximately-50-percent-compared-to-placebo-for-patients-with-mild-or-moderat/>. (e) Anon. Merck and Ridgeback Biotherapeutics Provide Update on Results from MOVE-OUT Study of Molnupiravir, an Investigational Oral Antiviral Medicine, in At Risk Adults With Mild-to-Moderate COVID-19, 2021. <https://www.merck.com/news/merck-and-ridgeback-biotherapeutics-provide-update-on-results-from-move-out-study-of-molnupiravir-an-investigational-oral-antiviral-medicine-in-at-risk-adults-with-mild-to-moderate-covid-19/>.

(11) (a) Beigel, J. H.; Tomashek, K. M.; Dodd, L. E.; Mehta, A. K.; Zingman, B. S.; Kalil, A. C.; Hohmann, E.; Chu, H. Y.; Luetkemeyer, A.; Kline, S.; et al. Remdesivir for the Treatment of Covid-19 - Final Report. *N. Engl. J. Med.* **2020**, *383*, 1813–1826. (b) De Crescenzo, F.; Amato, L.; Cruciani, F.; Moynihan, L. P.; D'Alò, G. L.; Vecchi, S.; Saule, R.; Mitrova, Z.; Di Franco, V.; Addis, A.; Davoli, M. Comparative Effectiveness of Pharmacological Interventions for Covid-19: A Systematic Review and Network Meta-Analysis. *Front. Pharmacol.* **2021**, *12*, No. 649472.

(12) (a) Rashad, A.; Mousa, S.; Nafady-Hego, H.; Nafady, A.; Elgendy, H. Short term survival of critically ill COVID-19 Egyptian patients on assisted ventilation treated by either Dexamethasone or Tocilizumab. *Sci. Rep.* **2021**, *11*, No. 8816. (b) Ranjbar, K.; Moghadami, M.; Mirahmadizadeh, A.; Fallahi, M. J.; Khaloo, V.; Shahriarirad, R.; Erfani, A.; Khodamoradi, Z.; Gholampoor Saadi, M. H. Methylprednisolone or dexamethasone, which one is superior corticosteroid in the treatment of hospitalized COVID-19 patients: a triple-blinded randomized controlled trial. *BMC Infect. Dis.* **2021**, *21*, No. 337.

(13) Richardson, P.; Griffin, I.; Tucker, C.; Smith, D.; Oechsle, O.; Phelan, A.; Rawling, M.; Savory, E.; Stebbing, J. Baricitinib as potential treatment for 2019-nCoV acute respiratory disease. *Lancet* **2020**, *395*, e30–e31.

(14) (a) Lenz, H. J.; Richardson, P.; Stebbing, J. The Emergence of Baricitinib: A Story of Tortoisoes Versus Hares. *Clin. Infect. Dis.* **2021**, *72*, 1251–1252. (b) Stebbing, J.; Krishnan, V.; de Bono, S.; Ottaviani, S.; Casalini, G.; Richardson, P. J.; Monteil, V.; Lauschke, V. M.; Mirazimi, A.; Youhanna, S.; et al. Mechanism of baricitinib supports artificial intelligence-predicted testing in COVID-19 patients. *EMBO Mol. Med.* **2020**, *12*, No. e12697.

(15) (a) Coelho, C.; Gallo, G.; Campos, C. B.; Hardy, L.; Wurtele, M. Biochemical screening for SARS-CoV-2 main protease inhibitors. *PLoS One* **2020**, *15*, No. e0240079. (b) Smith, E.; Davis-Gardner, M. E.; Garcia-Ordóñez, R. D.; Nguyen, T.-T.; Hull, M.; Chen, E.; Baillargeon, P.; Scampavia, L.; Strutzenberg, T.; Griffin, P. R.; et al. High-Throughput Screening for Drugs That Inhibit Papain-Like Protease in SARS-CoV-2. *SLAS Discovery* **2020**, *25*, 1152–1161. (c) Rothan, H. A.; Teoh, T. C. Cell-Based High-Throughput Screening Protocol for Discovering Antiviral Inhibitors Against SARS-COV-2 Main Protease (3CLpro). *Mol. Biotechnol.* **2021**, *63*, 240–248. (d) Gorshkov, K.; Chen, C. Z.; Xu, M.; Carlos de la Torre, J.; Martinez-Sobrido, L.; Moran, T.; Zheng, W. Development of a High-Throughput Homogeneous AlphaLISA Drug Screening Assay for the Detection of SARS-CoV-2 Nucleocapsid. *ACS Pharmacol. Transl. Sci.* **2020**, *3*, 1233–1241. (e) Chen, C. Z.; Shinn, P.; Itkin, Z.; Eastman, R. T.; Bostwick, R.; Rasmussen, L.; Huang, R.; Shen, M.; Hu, X.; Wilson, K. M.; et al. Drug Repurposing Screen for Compounds Inhibiting the Cytopathic Effect of SARS-CoV-2. *Front. Pharmacol.* **2020**, *11*, No. 592737. (f) Dittmar, M.; Lee, J. S.; Whig, K.; Segrist, E.; Li, M.; Kamalia, B.; Castellana, L.; Ayyanathan, K.; Cardenas-Diaz, F. L.; Morrissey, E. E.; et al. Drug repurposing screens reveal cell-type-specific entry pathways and FDA-approved drugs active against SARS-Cov-2. *Cell Rep.* **2021**, *35*, No. 108959.

(16) Hoffmann, M.; Kleine-Weber, H.; Schroeder, S.; Krüger, N.; Herrler, T.; Erichsen, S.; Schiergens, T. S.; Herrler, G.; Wu, N. H.;

Nitsche, A.; et al. SARS-CoV-2 Cell Entry Depends on ACE2 and TMPRSS2 and Is Blocked by a Clinically Proven Protease Inhibitor. *Cell* **2020**, *181*, 271–280.e278.

(17) Cao, L.; Goureshnik, I.; Coventry, B.; Case, J. B.; Miller, L.; Kozodoy, L.; Chen, R. E.; Carter, L.; Walls, A. C.; Park, Y. J.; et al. De novo design of picomolar SARS-CoV-2 miniprotein inhibitors. *Science* **2020**, *370*, 426–431.

(18) (a) Wu, Y.; Li, C.; Xia, S.; Tian, X.; Kong, Y.; Wang, Z.; Gu, C.; Zhang, R.; Tu, C.; Xie, Y.; et al. Identification of Human Single-Domain Antibodies against SARS-CoV-2. *Cell Host Microbe* **2020**, *27*, 891–898.e895. (b) Wrapp, D.; De Vlioger, D.; Corbett, K. S.; Torres, G. M.; Wang, N.; Van Breedam, W.; Roose, K.; van Schie, L.; VIB-CMB COVID-19 Response Team; Hoffmann, M.; et al. Structural Basis for Potent Neutralization of Betacoronaviruses by Single-Domain Camelid Antibodies. *Cell* **2020**, *181*, 1436–1441.

(19) Ekins, S.; Mottin, M.; Ramos, P. R. P. S.; Sousa, B. K. P.; Neves, B. J.; Foil, D. H.; Zorn, K. M.; Braga, R. C.; Coffee, M.; Southan, C.; et al. Déjà vu: Stimulating open drug discovery for SARS-CoV-2. *Drug Discovery Today* **2020**, *25*, 928–941.

(20) Premkumar, L.; Segovia-Chumbez, B.; Jadi, R.; Martinez, D. R.; Raut, R.; Markmann, A.; Cornaby, C.; Bartelt, L.; Weiss, S.; Park, Y.; et al. The receptor binding domain of the viral spike protein is an immunodominant and highly specific target of antibodies in SARS-CoV-2 patients. *Sci. Immunol.* **2020**, *5*, No. eabc8413.

(21) Gawriljuk, V. O.; Zin, P. P. K.; Puhl, A. C.; Zorn, K. M.; Foil, D. H.; Lane, T. R.; Hurst, B.; Tavella, T. A.; Costa, F. T. M.; Lakshmanane, P.; et al. Machine Learning Models Identify Inhibitors of SARS-CoV-2. *J. Chem. Inf. Model.* **2021**, *61*, 4224–4235.

(22) Puhl, A. C.; Fritch, E. J.; Lane, T. R.; Tse, L. V.; Yount, B. L.; Sacramento, C. Q.; Fintelman-Rodrigues, N.; Tavella, T. A.; Maranhão Costa, F. T.; Weston, S.; et al. Repurposing the Ebola and Marburg Virus Inhibitors Tilorone, Quinacrine, and Pyronaridine. *ACS Omega* **2021**, *6*, 7454–7468.

(23) Alves, J.; Engel, L.; de Vasconcelos Cabral, R.; Rodrigues, E. L.; de Jesus Ribeiro, L.; Higa, L. M.; da Costa Ferreira Júnior, O.; Castiñeiras, T. M. P. P.; de Carvalho Leitão, I.; Tanuri, A.; et al. A bioluminescent and homogeneous SARS-CoV-2 spike RBD and hACE2 interaction assay for antiviral screening and monitoring patient neutralizing antibody levels. *Sci. Rep.* **2021**, *11*, No. 18428.

(24) Lechuga, G. C.; Souza-Silva, F.; Sacramento, C. Q.; Trugilho, M. R. O.; Valente, R. H.; Napoleão-Pêgo, P.; Dias, S. S. G.; Fintelman-Rodrigues, N.; Temerozo, J. R.; Carels, N.; et al. SARS-CoV-2 Proteins Bind to Hemoglobin and Its Metabolites. *Int. J. Mol. Sci.* **2021**, *22*, No. 9035.

(25) (a) Santos, K. B.; Guedes, I. A.; Karl, A. L. M.; Dardenne, L. E. Highly Flexible Ligand Docking: Benchmarking of the DockThor Program on the LEADS-PEP Protein-Peptide Data Set. *J. Chem. Inf. Model.* **2020**, *60*, 667–683. (b) de Magalhães, C. S.; Barbosa, H. J. C.; Dardenne, L. E. A genetic algorithm for the ligand-protein docking problem. *Genet. Mol. Biol.* **2004**, *27*, 605–610. (c) de Magalhães, C. S.; Barbosa, H. J. C.; Dardenne, L. E. In *Selection-Insertion Schemes in Genetic Algorithms for the Flexible Ligand Docking Problem*, Genetic and Evolutionary Computation Conference; Springer: Berlin, Heidelberg, 2004.

(26) Toelzer, C.; Gupta, K.; Yadav, S. K. N.; Borucu, U.; Davidson, A. D.; Kavanagh Williamson, M.; Shoemark, D. K.; Garzoni, F.; Staufer, O.; Milligan, R.; et al. Free fatty acid binding pocket in the locked structure of SARS-CoV-2 spike protein. *Science* **2020**, *370*, 725–730.

(27) Madhavi Sastry, G.; Adzhigirey, M.; Day, T.; Annabhimoju, R.; Sherman, W. Protein and ligand preparation: parameters, protocols, and influence on virtual screening enrichments. *J. Comput.-Aided Mol. Des.* **2013**, *27*, 221–234.

(28) Anon. Schrödinger Release 2015-2: Protein Preparation Wizard; Schrödinger, L. Ed., 2015.

(29) Salentin, S.; Schreiber, S.; Haupt, V. J.; Adasme, M. F.; Schroeder, M. PLIP: fully automated protein-ligand interaction profiler. *Nucleic Acids Res.* **2015**, *43*, W443–W447.



- (30) Anon. Schrödinger. The PyMOL Molecular Graphics System, Version 1.8. Schrödinger, L. Ed., 2015.
- (31) Shoemark, D. K.; Colenso, C. K.; Toelzer, C.; Gupta, K.; Sessions, R. B.; Davidson, A. D.; Berger, I.; Schaffitzel, C.; Spencer, J.; Mulholland, A. J. Molecular Simulations suggest Vitamins, Retinoids and Steroids as Ligands of the Free Fatty Acid Pocket of the SARS-CoV-2 Spike Protein. *Angew Chem., Int. Ed.* **2021**, *60* (13), 7098–7110.
- (32) Ma, J.; Su, D.; Sun, Y.; Huang, X.; Liang, Y.; Fang, L.; Ma, Y.; Li, W.; Liang, P.; Zheng, S. Cryo-EM structure of S-Trimer, a subunit vaccine candidate for COVID-19. *J. Virol.* **2021**, DOI: [10.1128/JVI.00194-21](https://doi.org/10.1128/JVI.00194-21).
- (33) Gaulton, A.; Hersey, A.; Nowotka, M.; Bento, A. P.; Chambers, J.; Mendez, D.; Motow, P.; Atkinson, F.; Bellis, L. J.; Cibrian-Uhalte, E.; et al. The ChEMBL database in 2017. *Nucleic Acids Res.* **2017**, *45*, D945–D954.
- (34) Ellinger, B.; Bojkova, D.; Zaliani, A.; Cinatl, J.; Claussen, C.; Westhaus, S.; Keminer, O.; Reinshagen, J.; Kuzikov, M.; Wolf, M.; et al. et al. A SARS-CoV-2 cytopathicity dataset generated by high-content screening of a large drug repurposing collection. *Sci Data* **2021**, *8* (1), 70.
- (35) Olaleye, O. A.; Kaur, M.; Onyenaka, C.; Adebunsi, T. Discovery of Cloroquinol and analogues as novel inhibitors of Severe Acute Respiratory Syndrome Coronavirus 2 infection, ACE2 and ACE2 - Spike protein interaction in vitro. *Heliyon* **2021**, *7*, No. e06426.
- (36) Abian, O.; Ortega-Alarcon, D.; Jimenez-Alesanco, A.; Ceballos-Laita, L.; Vega, S.; Reyburn, H. T.; Rizzuti, B.; Velazquez-Campoy, A. Structural stability of SARS-CoV-2 3CLpro and identification of quercetin as an inhibitor by experimental screening. *Int. J. Biol. Macromol.* **2020**, *164*, 1693–1703.
- (37) Puhl, A. C.; Gomes, G. F.; Damasceno, S.; Godoy, A. S.; Noske, G. D.; Nakamura, A. M.; Gawriljuk, V. O.; Fernandes, R. S.; Monakhova, N.; Riabova, O. et al. Pyronaridine Protects Against SARS-CoV-2 in Mouse. *ACS Infect Dis*, 2022 DOI: [10.1101/2021.09.30.462449](https://doi.org/10.1101/2021.09.30.462449).
- (38) Anon. The Ukrainian company InterChem started clinical trials for the treatment of COVID-19 *Odessa J.*, 2020 <https://odessa-journal.com/interchem-started-clinical-trials-for-the-treatment-of-covid-19/>.
- (39) Oude Munnink, B. B.; Worp, N.; Nieuwenhuijse, D. F.; Sikkema, R. S.; Haagmans, B.; Fouchier, R. A. M.; Koopmans, M. The next phase of SARS-CoV-2 surveillance: real-time molecular epidemiology. *Nat. Med.* **2021**, *27*, 1518–1524.
- (40) Wrapp, D.; Wang, N.; Corbett, K. S.; Goldsmith, J. A.; Hsieh, C.-L.; Abiona, O.; Graham, B. S.; McLellan, J. S. Cryo-EM structure of the 2019-nCoV spike in the prefusion conformation. *Science* **2020**, *367*, 1260–1263.